JOC Article
pubs.acs.org/joc

Heterocyclic Annelated Di(perylene bisimide): Constructing Bowl-Shaped Perylene Bisimides by the Combination of Steric Congestion and Ring Strain

Hualei Qian,[†,§] Wan Yue,[†,§] Yonggang Zhen,[†,§] Simone Di Motta,[‡] Eugenio Di Donato,[‡] Fabrizia Negri,*[,‡] Jianqiang Qu,[∥] Wei Xu,[†] Daoben Zhu,[†] and Zhaohui Wang*[,†]

[†]*Beijing National Laboratory for Molecular Sciences, Key Laboratory of Organic Solids, Institute of Chemistry, Chinese Academy of Sciences,* [‡]*Dipartimento di Chimica "G. Ciamician", Unversità di Bologna, Via F. Selmi 2, 40126 Bologna, Italy, and INSTM, UdR Bologna, Italy,* [§]*Graduate School of the Chinese Academy of Sciences, Beijing 100190, China, and* [∥]*BASF Aktiengesellschaft, GVP/C-A030, 67056 Ludwigshafen, Germany*

wangzhaohui@iccas.ac.cn; fabrizia.negri@unibo.it

Received June 22, 2009

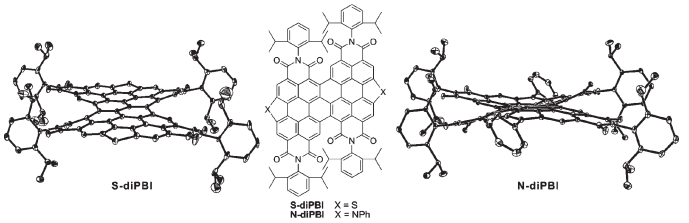

In this paper, we present the synthesis of S- and N-heterocyclic annelated di(perylene bisimide) with extraordinary doubly bowl-shaped structures. The structures of fused PBI bowls confirmed by single-crystal X-ray structure analysis and temperature-dependent ^{1}H NMR are realized by the introduction of the steric congestion in nonbay regions and by the concurrent formation of the five-membered heterorings strain in bay regions. On the basis of the geometry obtained from the X-ray analysis, the maximum POAV1 pyramidalization angle is found in N-heterocyclic annelated diPBI **7**, as large as 4.7°, indicating the formation of two PBI bowls with significant curvatures. Furthermore, to assist the electrochemical and spectroscopic characterization of the two bowl-shaped derivatives and to assess the influence of heteroatoms on the bowl curvature, quantum-chemically optimized atomic structures, electronic properties, and optical signatures were computed with density functional theory.

Introduction

The immense interest surrounding fullerenes has directed increasing attention toward bowl-shaped polycyclic aromatic hydrocarbons (PAHs), also called molecular bowls, and these have become attractive targets for design and synthesis.[1] In recent years, various molecular bowls, displaying curved molecular structures and π-surfaces, extraordinary chemical and physical properties, and unique self-assembly behavior, have been prepared by either flash vacuum pyrolysis (FVP)[2] or wholly solution-phase synthetic methods.[3] Incorporation of heteroatoms into curved PAHs has been shown to determine several intriguing properties associated with the modified π-electron systems and the potential applications.[4] However, up to now, there have

*To whom correspondence should be addressed.

(1) (a) Rabideau, P. W.; Sygula, A. *Acc. Chem. Res.* **1996**, *29*, 235–242. (b) Wu, Y.; Siegel, J. S. *Chem. Rev.* **2006**, *106*, 4843–4867. (c) Tsefrikas, V. M.; Scott, L. T. *Chem. Rev.* **2006**, *106*, 4868–4884. (d) Kawase, T.; Kurata, H. *Chem. Rev.* **2006**, *106*, 5250–5273.

(2) (a) Scott, L. T.; Boorum, M. M.; Mcmahon, B. J.; Hagen, S.; Mack, J.; Blank, J.; Wegner, H.; Meijere, A. D. *Science* **2002**, *295*, 1500–1503. (b) Bronstein, H. E.; Choi, N.; Scott, L. T. *J. Am. Chem. Soc.* **2002**, *124*, 8870–8875.

(3) (a) Sygula, A.; Rabideau, P. W. *J. Am. Chem. Soc.* **1999**, *121*, 7800–7803. (b) Seiders, T. J.; Elliott, E. L.; Grube, G. H.; Siegel, J. S. *J. Am. Chem. Soc.* **1999**, *121*, 7804–7813. (c) Sakurai, H.; Daiko, T.; Hirao, T. *Science* **2003**, *301*, 1878.

(4) (a) Bendikov, M.; Wudl, F. *Chem. Rev.* **2004**, *104*, 4891–4945. (b) Anthony, J. E. *Chem. Rev.* **2006**, *106*, 5028–5048. (c) Wu, Y.; Li, Y.; Gardner, S.; Ong, B. S. *J. Am. Chem. Soc.* **2005**, *127*, 614–618.

DOI: 10.1021/jo901285k Published on Web 07/06/2009

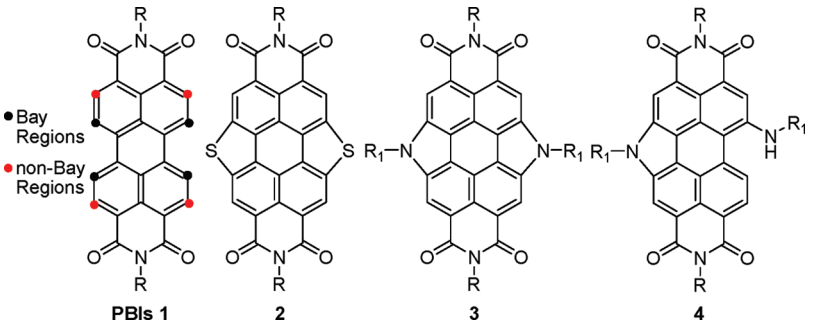

FIGURE 1. PBIs **1**, S-PBI **2**, and N-PBIs **3** and **4**.

been only a few reports on strained aromatic polycycles including heteroatoms such as S and N in their frameworks.[5]

Perylene-3,4:9,10-tetracarboxylbisimides **1** (PBIs) have been intensively investigated primarily in industry as dyes and pigments[6] and recently in electronics and optoelectronics as important n-type materials.[7] The extensive interest in PBIs is due to the versatile optical and electrochemical properties, the controllable structures and properties, the chemical and thermal stabilities, and the high electron affinity.[8] The two different types of positions in the aromatic core of PBIs, namely the bay regions and the nonbay regions, are depicted in Figure 1. Modifications of PBIs have been concentrated on the bay regions, whose chemical substitution can dramatically alter the optical and electronic properties. Notably, substituents in bay regions can twist the perylene unit dihedrally out of plane, leading to the dihedral angle being easily tunable from 0° to 37°.[9] Despite this documented flexibility in the bay region, PBIs with curved π-structures have been rarely explored. The incorporation of bowl-shaped structures to n-type chromophores can significantly change intermolecular interactions, chemical and physical properties, and possible applications.

As numerous examples prove the importance of five-membered rings in the formation of bowl-shaped structures, our initial strategy for PBI bowls was based on introducing heteroring strain into two bay regions and using the stress strain to form curved structures. Thus, we attempted to prepare **2** and **3** by the incorporation of two thiophene and pyrrole rings, respectively. However, the crystal structure of **2** previously reported by our group reveals a planar perylene core probably because of the long length of C−S bonds (1.78 Å) and, as a consequence, the weak ring strain.[10] In contrast with **2**, the DFT optimized structure of **3** shows a deeply bowl-shaped configuration (see Figure S6 in the Supporting Information) due to the strong strain resulting from the short length of C−N bonds (1.41 Å). We expected to synthesize **3** by the Buchwald−Hartwig reaction[11] of tetrahalogen-PBIs with an amine. The only observed product was **4** instead of **3** (Supporting Information), indicating the high energy needed for simultaneously forming two strained pyrrole rings in bay regions. These findings demonstrate the difficulty in preparing a PBI bowl by modifying the bay regions, suggesting that an extended aromatic system may be necessary for flexibility and to reduce the energy costs of making the five-membered ring.

The influence of nonbay regions on structures and properties of **1** has been neglected mainly because of the difficulty in modulating PBIs in nonbay regions. Recently, we reported the CuI-mediated synthesis of di(perylene bisimides) **5** (diPBIs),[12] which is the first example demonstrating the participation of the C−H bond in the nonbay region to the reaction, and thus it can be regarded as an ideal platform for investigating the effect of nonbay regions on structures. It has been demonstrated, by the computed structures of **5** and their extended trimers, that the steric congestion between H atoms in the nonbay region and the adjacent O atoms (blue label in **5** shown in Figure 2) twists the aromatic core to an out-of-plane configuration.[13] Accordingly, we modified our strategy for the design of PBI bowls, first by introducing the steric congestion in nonbay regions through the synthesis of diPBIs and second by including the strained heterorings in bay regions. Herein we present the synthesis of S- and N-heterocyclic annelated diPBIs **6** and **7**, and confirm their doubly bowl-shaped structures by single-crystal X-ray structure analysis and temperature-dependent ^{1}H NMR. Furthermore, the influence of heteroatoms on the bowl curvature, the optical signatures, and electrochemical properties have been experimentally determined and rationalized on the basis of quantum-chemically computed atomic structures, electronic properties, and optical signatures.

(5) (a) Imamura, K.; Takimiya, K.; Aso, Y.; Otsubo, T. *Chem. Commun.* **1999**, 1859–1860. (b) Mascal, M.; Lera, M.; Blake, A. J. *J. Org. Chem.* **2000**, *65*, 7253–7255. (c) Mascal, M.; Bertran, J. C. *J. Am. Chem. Soc.* **2005**, *127*, 1352–1353.

(6) (a) Herbst, W.; Hunger, K. *Industrial Organic Pigments: Production, Properties, Applications*, 2nd ed.; WILEY-VCH: Weinheim, Germany, 1997. (b) Zollinger, H. *Color Chemistry*, 3rd ed.; VCH: Weinheim, Germany, 2003.

(7) (a) Schmidt-Mende, L.; Fechtenkötter, A.; Müllen, K.; Moons, E.; Friend, R. H.; Mackenzie, J. D. *Science* **2001**, *293*, 1119–1122. (b) Ego, C.; Marsitzky, D.; Becker, S.; Zhang, J.; Grimsdale, A. C.; Müllen, K.; Mackenzie, J. D.; Silva, C.; Friend, R. H. *J. Am. Chem. Soc.* **2003**, *125*, 437–443. (c) Jones, B. A.; Ahrens, M. J.; Yoon, M.; Facchetti, A.; Marks, T. J.; Wasielewski, M. R. *Angew. Chem., Int. Ed.* **2004**, *43*, 6363–6366. (d) Schmidt, R.; Ling, M. M.; Oh, J. H.; Winkler, M.; Könemann, M.; Bao, Z.; Würthner, F. *Adv. Mater.* **2007**, *19*, 3692–3695.

(8) (a) Würthner, F. *Chem. Commun.* **2004**, 1564–1579. (b) Wasielewski, M. R. *J. Org. Chem.* **2006**, *71*, 5051–5066. (c) Watson, M. D.; Fechtenkotter, A.; Müllen, K. *Chem. Rev.* **2001**, *101*, 1267–1300.

(9) (a) Hadicke, E.; Graser, F. *Acta Crystallogr., Sect. C* **1986**, *42*, 189–195. (b) Chen, Z.; Debije, M. G.; Debaerdemaeker, T.; Osswald, P.; Würthner, F. *ChemPhysChem* **2004**, *5*, 137–140. (c) Osswald, P.; Leusser, D.; Stalke, D.; Würthner, F. *Angew. Chem., Int. Ed.* **2005**, *44*, 250–253. (d) Shaller, A. D.; Wang, W.; Gan, H.; Li, A. D. Q. *Angew. Chem., Int. Ed.* **2008**, *47*, 7705–7709. (e) Wang, W.; Shaller, A. D.; Li, A. D. Q. *J. Am. Chem. Soc.* **2008**, *130*, 8271–8279. (f) Li, Y.; Tan, L.; Wang, Z.; Qian, H.; Shi, Y.; Hu, W. *Org. Lett.* **2008**, *10*, 529–532.

(10) Qian, H.; Liu, C.; Wang, Z.; Zhu, D. *Chem. Commun.* **2006**, 4587–4589.

(11) Ackermann, L.; Althammer, A. *Angew. Chem., Int. Ed.* **2007**, *46*, 1627–1629.

(12) Qian, H.; Wang, Z.; Yue, W.; Zhu, D. *J. Am. Chem. Soc.* **2007**, *129*, 10664–10665.

(13) Qian, H.; Negri, F.; Wang, C.; Wang, Z. *J. Am. Chem. Soc.* **2008**, *130*, 17970–17976.

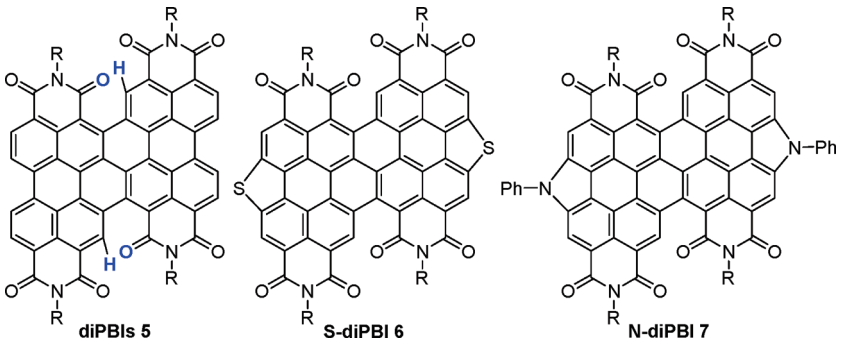

FIGURE 2. DiPBIs **5**, S-diPBI **6**, and N-diPBI **7**.

SCHEME 1. Synthesis of S-diPBI 6 and N-diPBI 7[a]

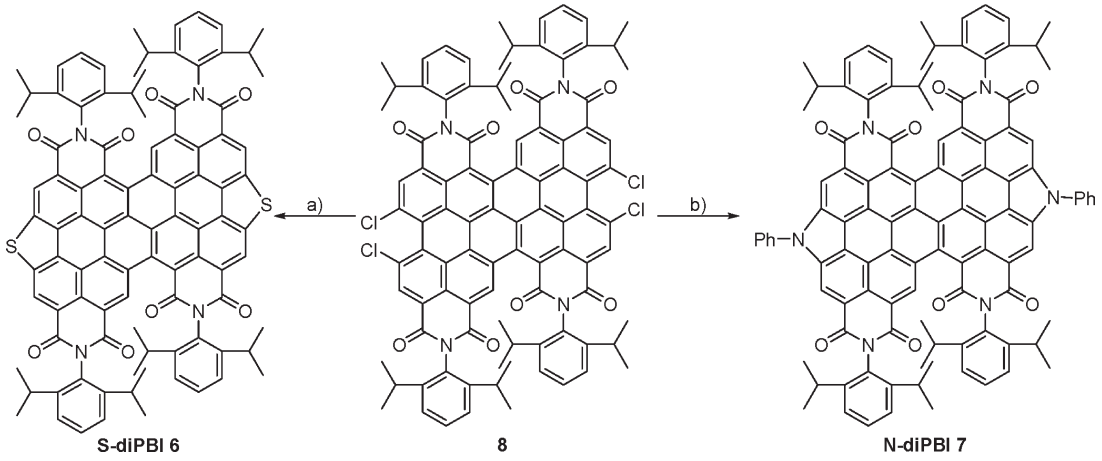

[a]Conditions and reagents: (a) $Bu^3SnSSnBu_3$, $Pd(PPh_3)_4$, toluene, reflux, 12 h, 68%; (b) $Pd(OAc)_2$, PCy_3, $PhNH_2$, KOtBu, toluene, reflux, 5 h, 51%.

Results and Discussion

Computational Details. Atomic structures of **3**, **5**, **6**, and **7** were optimized with density functional theory (DFT) calculations, using the B3LYP hybrid functional[14] with the basis set limited to 3-21G* owing to the large dimension of the chromophores. Molecular orbital shapes and energies of **6** and **7** discussed in the text are those calculated at the optimized cis structures. Orbital pictures were prepared with Molekel 4.3 visual software.[15] Electronic excitation energies and oscillation strengths were computed for the 60 lowest singlet excited electronic states of **6** and **7** with time-dependent (TD) DFT calculations. In plotting computed electronic spectra, a Lorentzian line width of 0.1 eV was superimposed to each computed intensity to facilitate the comparison with experimental spectra. The computed spectra did not include the vibronic structure associated with electronic bands and as a result they show a reduced number of bands compared with the experimental spectra. All quantum-chemical calculations were performed with the Gaussian03 package.[16]

Synthesis and Optimized Structures. Following our strategy, we attempted to prepare S- and N-heterocyclic annelated diPBIs by Stille-type and Buchwald−Hartwig reaction, which have been widely employed in the formation of C−S[17] and C−N[18] bonds, respectively. Accordingly, S-heterocyclic annelated diPBI **6** (S-diPBI) was obtained as blue-black solids in a high yield of 68% by the $Pd(PPh_3)_4$-catalyzed reaction of **8** with $Bu_3SnSSnBu_3$,[10] and N-heterocyclic annelated diPBI **7** (N-diPBI) as green-black solids in a yield of 51% by the $Pd(OAc)_2$-catalyzed reaction[11] of **8** with aniline (Scheme 1). The structures of **6** and **7** were verified by ^1H NMR, ^{13}C NMR spectroscopy, and MALDI-TOF. Moreover, the synthetic protocol discussed above reveals that the formation of two pyrrole rings in the bay regions of diPBIs is much easier than that for PBIs. A likely reason is the energetically more favorable formation of five-member rings in the extended aromatic system.

For the diPBI series, the steric congestion between oxygen and the neighboring hydrogen atom is expected to result in two possible conformers, namely, the trans and cis conformer, in which both ends of each PBI unit tilt in different and the same direction, respectively. To investigate the effect of the steric congestion and the heterorings strain on structures,

(14) (a) Becke, A. D. *Phys. Rev. A* **1988**, *38*, 3098–3100. (b) Lee, C.; Yang, W.; Parr, G. G. *Phys. Rev. B* **1988**, *37*, 785–789.

(15) *Molekel*, version 4.3, http://www.cscs.ch/molkel/; Portmann, S.; Lüthi, H. P. *Chimia* **2000**, *54*, 766.

(16) Frisch, M. J.; et al. *Gaussian 03*, revision C.02; Gaussian, Inc., Pittsburgh, PA, 2003.

(17) (a) Kosugi, M.; Ogata, T.; Terada, M.; Sano, H.; Migita, T. *Bull. Chem. Soc. Jpn.* **1985**, *58*, 3657–3658. (b) Zhang, X.; Côté, A. P.; Matzger, A. J. *J. Am. Chem. Soc.* **2005**, *127*, 10502–10503.

(18) (a) Hartwig, J. F. In *Handbook of Organopalladium Chemistry for Organic Synthesis*; Negishi, E. I., de Meijere, A., Eds.; Wiley-Interscience: Weinheim, Germany, 2002. (b) Jiang, L.; Buchwald, S. L. In *Metal-Catalyzed Cross-Coupling Reactions*, 2nd ed.; de Meijere, A., Diederich, F., Eds.; John Wiely & Sons: Weinheim, Germany, 2004.

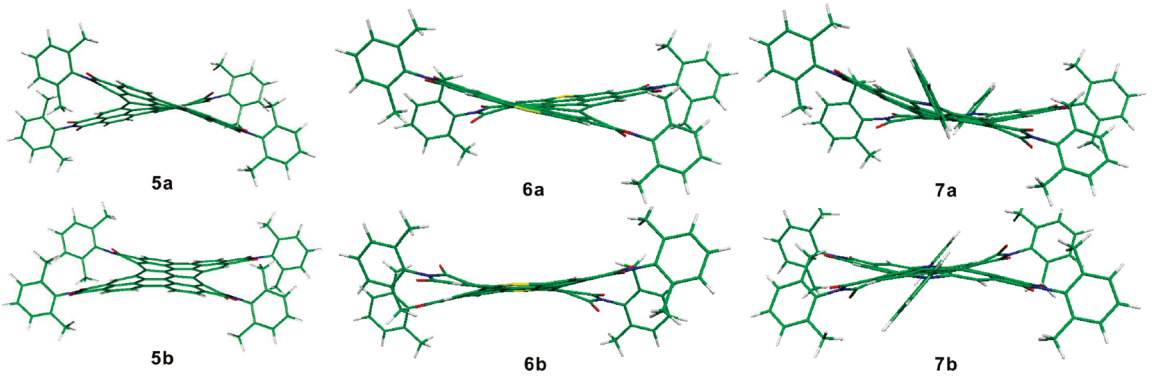

FIGURE 3. Equilibrium structures of trans (a) and cis (b) conformers of **5**, **6**, and **7** computed at the B3LYP/3-21G* level.

quantum chemical calculations were carried out on models for **6** and **7** as well as **5** for comparison, featuring methyl substituents instead of the isopropyl units on the phenyl rings.

For **5**−**7**, low-energy trans and cis conformers were optimized, representing two different out-of-plane deformations of the two PBI moieties (Figure 3). As shown in Figure 3, PBI moieties in the trans conformer of **5** are planar, while in the cis conformer, their aromatic cores are forced to be bent by the steric congestion in nonbay regions. In the trans conformer of **6**, the aromatic core of each PBI unit is almost planar, while in the cis conformer, the PBI moieties exhibit a shallow bowl-shaped structure. In contrast with the trans conformer of **6**, each PBI unit in the trans structure of **7** is twisted, and compared to the cis conformer of **6**, the bowl shape of the PBI moieties in the cis structure of **7** is strongly enhanced. These changes are justified by the larger strain induced by pyrrole rings with respect to thiophene rings. Notably, for S- and N-diPBI, the computed energies of trans and cis configurations are much closer than those of diPBI **5** (see Table S1 in the Supporting Information), indicating that the incorporation of S and N atoms increases the stability of cis conformers while decreasing that of trans conformers, leading ultimately to a more stable cis conformer for **7**.

Single-Crystal Structures and Bowl Curvatures. Crystals of S- and N-diPBI suitable for single-crystal X-ray structure analysis are obtained at room temperature. As revealed by the crystal structures of **6** and **7** (Figure 4), only cis conformers are found in the obtained single crystals. To determine whether the trans conformers are contained in the products, we did the temperature-dependent ^{1}H NMR experiments of **6** and **7** in $CDCl_3$ (Supporting Information) and only observed slight changes in the chemical shift of aromatic protons, which correspond to the same isomeric form and are possibly due to vibrational cooling effects. The temperature-dependent ^{1}H NMR spectra of both **6** and **7** did not show a trace of the presence of two isomers. Thus, as proved by the crystal structures and the temperature-dependent ^{1}H NMR experiments, only the cis conformers of **6** and **7** were obtained in the products of Stille-type and Buchwald reactions.

The crystal structures of S-diPBI **6** and N-diPBI **7** reveal that both of them have crystallographically imposed inversion symmetry and the steric congestion between H atoms in nonbay regions and the adjacent O atoms force the neighboring imide rings to adopt an out-of-plane distorted conformation (Figure 4). With the steric congestion in nonbay regions and the strain induced by the five-membered rings in bay regions, each PBI unit in **6** and **7**, containing perylene rings with a fused heteroring, exhibits extraordinary bowl-shaped structures. For both **6** and **7**, the two PBI bowls opening in opposite directions are fully conjugated via the three C−C bonds in the center. Moreover, the PBI bowls in **6** are much shallower than those in **7**, indicating that the strain induced by C−S bonds (length: 1.76 Å) in thiophene rings is weaker than that by C−N bonds (length: 1.41 Å) in pyrrole rings, in close agreement with the computed C-heteroatom bond lengths (Supporting Information). Notably, for each PBI bowl in the crystal structure of **7**, one acetone molecule is on the convex side with a nonbonding C···O distance of 3.12 Å and two CH_2Cl_2 molecules on the concave side with nonbonding C···Cl distances of 3.27 and 3.45 Å, respectively (see Figure S8 in the Supporting Information).

The curvature was evaluated by the method of π-orbital axis vector analysis (POAV1)[19] based on the geometry obtained from the X-ray analysis. In S-diPBI, the highest local curvature, 2.9°, is found on C19 (C19A) that are in the imide rings, and the average pyramidalization angle for the carbons of the central benzene ring in the perylene core is 1.0°. Compared with **6**, the pyramidalization angles for most carbons in the aromatic core of **7** are much higher, indicating the strongly enhanced bowl-shaped structures induced by pyrrole rings. As shown by the crystal structure of **7**, the highest local curvature, 4.7°, is found on C10 (C10A), corresponding to one of the β-carbons in the pyrrole rings, and the average pyramidalization angle for the carbons of the central benzene ring in the perylene core is 3.1°. These results are in agreement with the computed structures (Supporting Information) and the POAV1 analysis provides further evidence on the enhanced bowl-shaped structure of **7** compared to that of **6**, induced by the increased strain associated with pyrrole rings. It is also suggested that the curvatures of PBI bowls in the diPBI series can be easily modified by the introduction of atoms with different radius in bay regions.

Not only do they significantly alter the structures of the aromatic core, but the introduction of heteroatoms to diPBI skeletons also induces highly ordered superstructures. Interestingly, unique ribbons of S-diPBI **6** were observed in the crystal structure (Figure 5), similarly with those found in the

(19) (a) Haddon, R. C.; Scott, L. T. *Pure Appl. Chem.* **1986**, *58*, 137–142. (b) Haddon, R. C. *J. Am. Chem. Soc.* **1987**, *109*, 1676–1685. (c) Haddon, R. C. *Science* **1993**, *261*, 1545–1550.

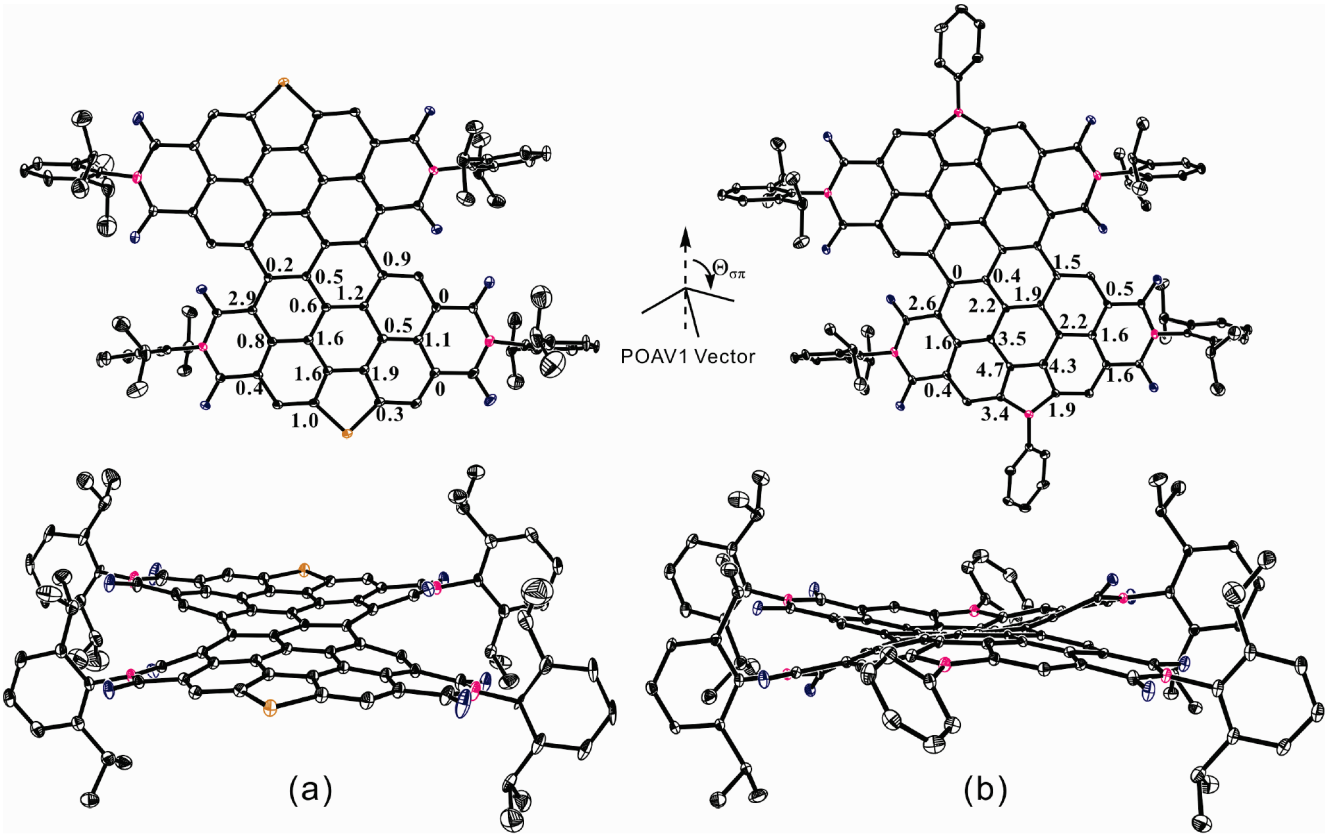

FIGURE 4. ORTEP drawing of the molecular structures of **6** (a) and **7** (b) with 30% probability ellipsoids. POAV1 pyramidalization angles ($\Theta_{\sigma\pi} - 90$) of one PBI unit based on the crystal structures of **6** and **7** are given: (top) top view and (bottom) side view.

crystal of **2**. The inversion-related pairs of S-diPBI molecules in the crystal of **6** are linked by C3−H3···O1 hydrogen bonds with H···O distances of 2.29 Å and C−H···O 134.7° and S1···O1 intermolecular contacts with S···O distances of 3.06 Å. The probable reason for the formation of ribbons in **6** is the subtle influence of sulfur atoms on the molecular electronic structure.

Absorption Spectra and Electrochemical Properties. The introduction of S and N atoms to diPBI skeletons leads to a remarkable change in the electronic absorption spectra. The blue-black solution of S-diPBI **6** exhibits three major absorption bands at 411, 584, and 633 nm ($\varepsilon_{max} = 90\,500\ M^{-1}\ cm^{-1}$) with a blue shift of 51 nm relative to **5**, as a reflection of the expanded aromatic core (Figure 6) with a five-atom ring. Compared with **5**, N-diPBI **7** displays hypsochromically shifted spectra with five major bands at 414, 430, 574, 620, and 670 nm ($\varepsilon_{max} = 77\,100\ M^{-1}\ cm^{-1}$). As revealed by the absorption spectra, the energy of the lowest allowed electronic transition, namely the optical gap, increases with the incorporation of heteroatoms in bay regions.

The TDDFT calculated absorption spectra of **6** and **7** agree very well with the observed counterpart although the excitation energy of the $S_0 \rightarrow S_1$ transition of **7** is overestimated. The overestimate results from the limited basis set we were forced to use because of the size of the systems. Calculations on similar heteroderivatives of smaller sizes show that an almost perfect match between computed and observed energies is obtained employing the larger 6-31 + G** basis set.

The comparison between computed and observed spectra shows an interesting feature characterizing the bowl-shaped heteroderivatives featuring five-member rings. The shallow maximum observed for **5** at ca. 510−520 nm (black dot in the figure) disappears for **6** and **7** and at the same time a new electronic transition appears at lower energies (red and blue triangles in the figure), in the region of the 0−1 vibronic band associated with the first electronic transition. Inspection of the wave functions associated with these (black dot and red, blue triangles) electronic transitions shows a similar orbital nature. The red shift in bowl-shaped derivatives results from the modulation of molecular orbital energies (and shapes) induced by the presence of the heteroatoms forming the five-member rings.

The frontier orbitals (the highest occupied and the lowest two unoccupied) of **6** and **7** at the optimized cis structures, along with a schematic representation of their computed energies, are depicted in Figure 7. It can be seen that the incorporation of heteroatoms modifies the shapes of these orbitals compared with those of **5** (see Figure S13 in the Supporting Information) although they conserve essentially the same parentage. The energies of LUMO and LUMO + 1 of **6** and **7** are less negative than those of **5** because of the expanded π-system by heteroatoms.

Similar to **5**, the cyclic voltammograms of **6** and **7** exhibit four reduction waves (Figure 8), revealing that both **6** and **7** are easily reduced and can accept up to four electrons. The half-wave reduction potentials vs. Fc/Fc^+ are −0.62, −0.90, −1.60, and −1.73 V for **6** and −0.73, −1.01, −1.65, and −1.85 V for **7**. Compared with **5**,[12] the first reduction potentials of **6** and **7** are more negative, suggesting an increased LUMO energy associated with the expansion of

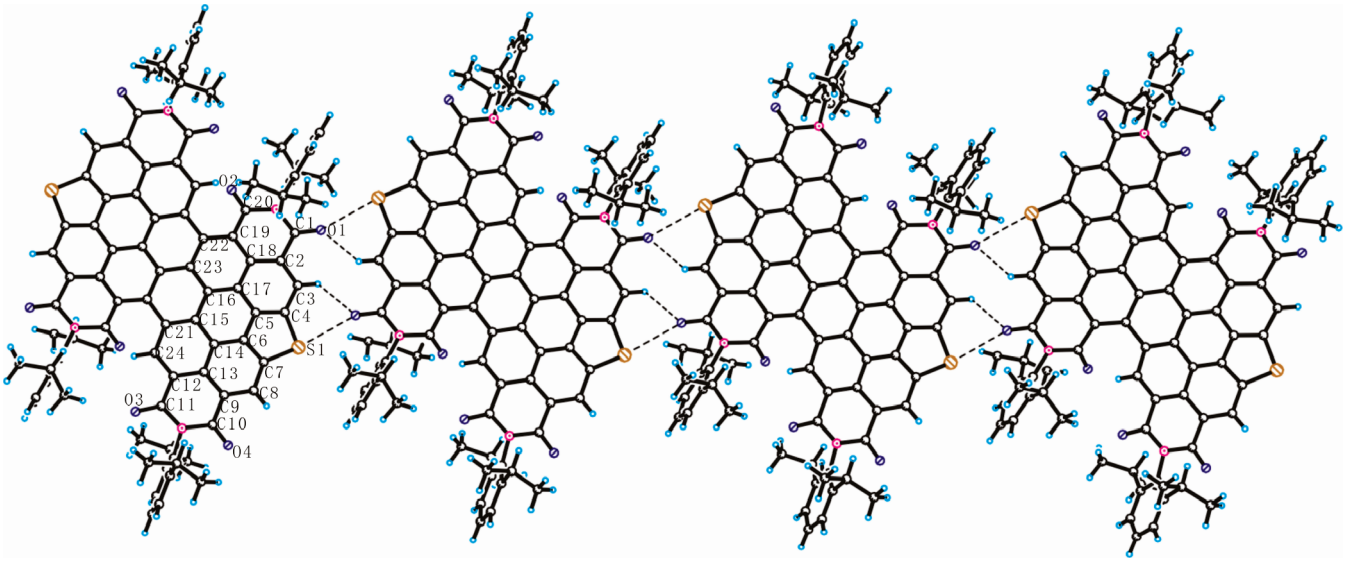

FIGURE 5. Intermolecular interactions in the crystal structure of **6**.

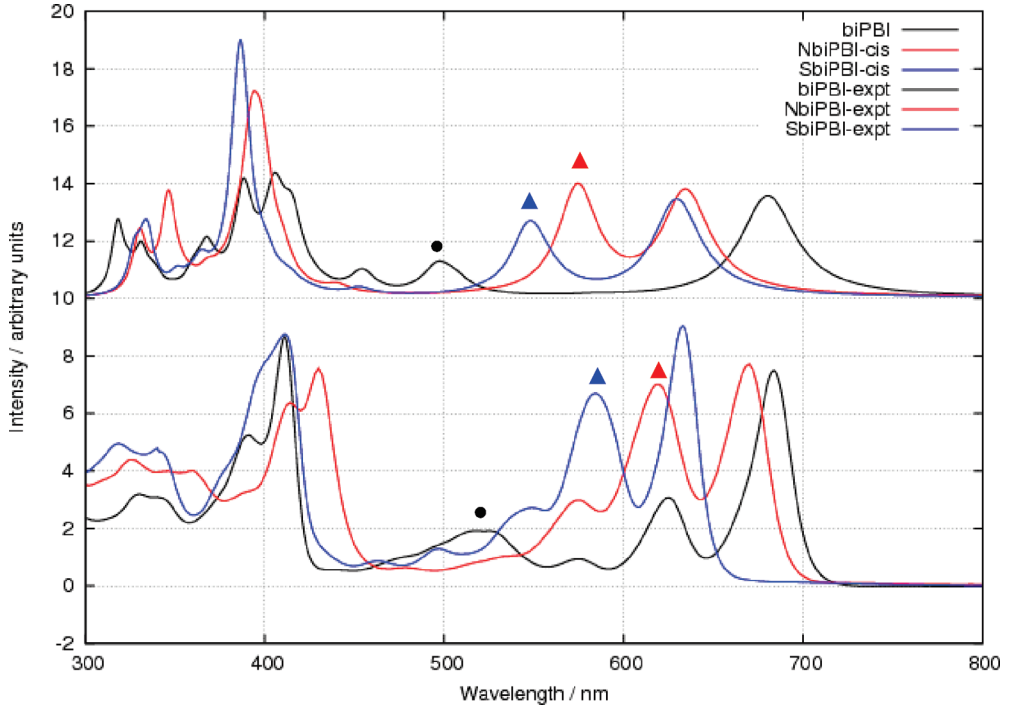

FIGURE 6. Top: The TD B3LYP/3-21G* calculated absorption spectra of **5** (black), **6** (blue), and **7** (red) at the optimized cis structures. Bottom: Absorption spectra of **5** (black), **6** (blue), and **7** (red) in $CHCl_3$.

the conjugated system through the incorporation of a pentagonal ring, in agreement with the computed results (see Table S1 in the Supporting Information). Due to the stronger electron-donating properties of nitrogen atoms compared to sulfur atoms, **7** is more difficult to reduce than **6**, in agreement with the calculated LUMO energies. Thus, the electrochemical properties as well as the frontier orbital energies can be easily modulated by incorporating different heteroatoms into bay regions of diPBI.

Conclusions

In summary, we have presented the facile synthesis of S- and N-diPBI with extraordinary doubly bowl-shaped structures. The structures of PBI bowls confirmed by single-crystal X-ray structure analysis are realized by the introduction of the steric congestion in nonbay regions between hydrogen atoms and neighboring oxygen atoms and by the concurrent formation of the five-membered heterorings strain in bay regions. Moreover, on the basis of the geometry obtained from the X-ray analysis of **6** and **7**, the maximum pyramidalization angle is found in **7**, as large as 4.7°, indicating the formation of two PBI bowls with significant curvatures. The analysis of the absorption spectra has revealed a unique fingerprint associated with the presence of pentagon rings, a marked red shift of the second allowed electronic transition. Furthermore, the curvatures, the electronic properties, and the frontier orbitals

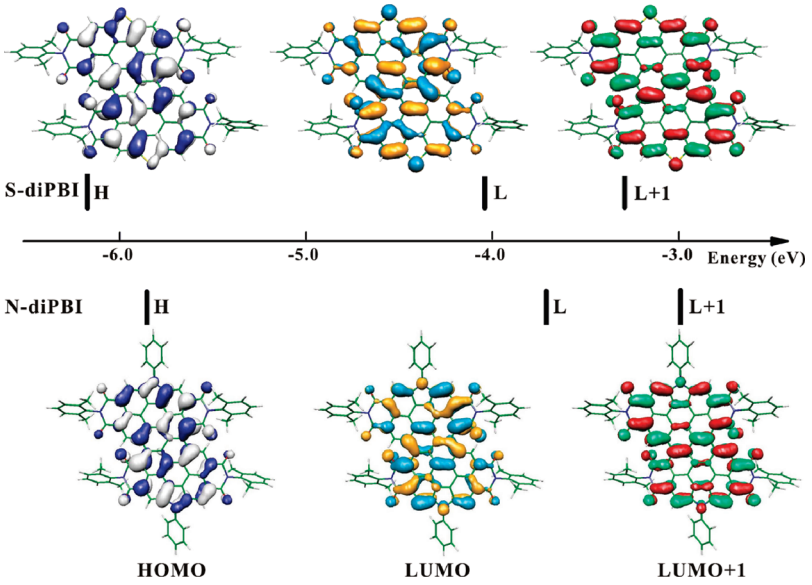

FIGURE 7. B3LYP/3-21G* computed energies and shapes of the frontier orbitals of S-diPBI **6** (top) and N-diPBI **7** (bottom) at the optimized cis structure.

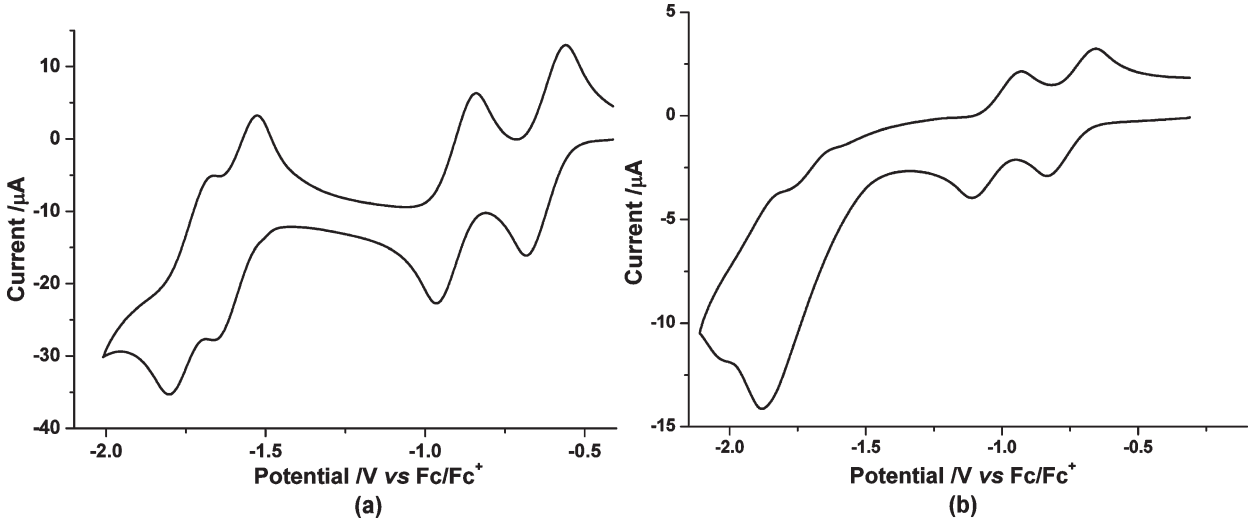

FIGURE 8. Reductive cyclic voltammograms of **6** (a) and **7** (b) in CH_2Cl_2. Scan rate: 0.1 V/s (electrolyte: 0.1 M $TBAPF_6$).

of the PBI bowls can be easily modulated by altering the covalent radius of the bridged atoms. In light of the accessibility to synthesis and functionalization, the unique doubly bowl-shaped structures, the controllable curvatures, and the easily tunable optical and electrochemical properties, heterocyclic annelated diPBIs are promising not only for basic research in molecular engineering, but also for applications in materials science.

Experimental Section

Synthesis and Characterization. All chemicals were purchased from commercial suppliers and used without further purification unless otherwise specified. Toluene was freshly distilled from sordium prior to use. Tetrachloro-diPBIs **8** were prepared according to known procedures.[12]

S-diPBI 6. $Pd(PPh_3)_4$ (156 mg, 0.135 mmol) and $Bu_3SnSSnBu_3$ (552 mg, 0.90 mmol) were added to a solution of **8** (700 mg, 0.45 mmol) in toluene under Ar. The mixture was refluxed for 12 h. After removal of the solvent under vacuum, the crude was washed with EtOH, dried, dissolved in dichloromethane, and purified by column chromatography (silica gel, petroleum ether/CH_2Cl_2 = 1:3). Yield 451 mg (68%) of **6** as a blue-black solid. ^{1}H NMR ($CDCl_3$, 300 MHz, 298 K, TMS) δ 10.88 (s, 2H), 10.20 (s, 2H), 9.93 (s, 2H), 7.54 (m, 4H), 7.40 (d, ^3J(H,H) = 7.8 Hz,8H), 3.15 (br, 4H), 2.90 (m, 4H), 1.28 (m, 24H), 1.13 (d, ^3J(H,H) = 6.8 Hz, 12H), 0.87 (d, ^3J(H,H) = 6.7 Hz, 12H); ^{13}C NMR ($CDCl_3$, 150 MHz, 298 K) δ 164.9, 164.7, 164.6, 163.4, 146.2, 146.1, 140.4, 139.7, 132.0, 131.8, 131.6, 131.5, 131.3, 129.3, 127.3, 125.9, 125.8, 125.0, 124.4, 123.3, 123.1, 121.6, 121.5, 120.1, 119.4, 29.9, 29.4, 24.7, 24.3, 24.2, 24.1. MS (MALDI-TOF) calcd for M^- 1474.5, found 1474.9.

N-diPBI 7. Aniline (110 mg, 1.18 mmol) was added to a mixture of tetrachloro-diPBIs **8** (250 mg, 0.16 mmol), $Pd(OAc)_2$ (80 mg, 0.36 mmol), PCy_3 (70 mg, 0.25 mmol), and KO*t*-Bu (200 mg, 1.79 mmol) in 10 mL of toluene under Ar. The mixture was refluxed for 5 h, and then cooled. After removal of the solvent under vacuum, the crude was washed with HCl and extracted with CH_2Cl_2. The organic layers were separated,

washed with brine, dried over Na_2SO_4, and purified by column chromatography (silica gel, CH_2Cl_2). Yield 130 mg (51%) of **7** as a black solid. ^{1}H NMR (CD_2Cl_2, 300 MHz, 298 K, TMS) δ 10.93 (s, 2H), 9.80 (s, 2H), 9.51 (s, 2H), 8.19 (d, ^3J(H,H) = 7.8 Hz, 4H), 7.86 (t, ^3J(H,H) = 7.8 Hz, 4H), 7.67 (m, 4H), 7.51 (m, 2H), 7.38 (m, 8H), 3.17 (m, 4H), 2.86 (m, 4H), 1.31 (d, ^3J(H,H) = 6.7 Hz, 12H), 1.14 (d, ^3J(H,H) = 6.6 Hz, 12H), 1.08 (m, 24H). ^{13}C NMR (CD_2Cl_2, 100 MHz, 298 K) δ 165.9, 165.5, 164.6, 146.5, 138.1, 137.1, 132.3, 131.1, 130.2, 128.5, 125.9, 125.5, 124.9, 124.5, 123.9, 123.2, 122.8, 121.6, 121.3, 120.5, 119.4, 29.8, 29.2, 22.8. MS (MALDI-TOF) calcd for M^- 1592.6, found 1592.4.

Crystallographic Data. S-diPBI 6:. 0.5S-diPBI·0.75CH_2Cl_2·C_6H_{14}, $C_{54.75}H_{52.50}Cl_{1.50}N_2O_4S$, M_w = 887.72, triclinic, space group $P\bar{1}$, a = 8.3321(14) Å, b = 15.291(3) Å, c = 20.134(4) Å, α = 73.673(4)°, β = 86.124(6)°, γ = 85.033(6)°, V = 2450.1(7) Å^3, Z = 2, D_c = 1.203 g/cm^3, μ = 0.194 mm^{-1}, θ range 1.97−25.00°. Of the 8605 reflections that were collected, 7110 were unique (R_{int} = 0.0346), GOF = 1.285, R_1 = 0.0962, wR_2 = 0.2987 for reflections with $I > 2\sigma(I)$. Largest diff. peak and hole, 1.423 and −1.126 e/Å^3.

N-diPBI 7:. 0.5N-diPBI·4CH_2Cl_2·C_3H_6O, $C_{61}H_{56}Cl_8N_3O_5$, M_w = 1194.69, monoclinic, space group $P121/a1$, a = 18.270(2) Å, b = 16.5555(17) Å, c = 19.663(3) Å, α = 90.00°, β = 101.596(6)°, γ = 90.00°, V = 5826.2(12) Å^3, Z = 4, D_c = 1.362 g/cm^3, μ = 0.438 mm^{-1}, θ range 1.62−25.00°. Of the 10255 reflections that were collected, 9157 were unique (R_{int} = .0.0685), GOF = 1.191, R_1 = 0.0959, wR_2 = 0.2568 for reflections with $I > 2\sigma(I)$. Largest diff. peak and hole, 0.803 and −0.934 e/Å^3.

Acknowledgment. For financial support of this research, we thank the National Natural Science Foundation of China (grant nos. 20721061 and 50873106), 973 Program (Grant 2006CB932101), Chinese Academy of Sciences, BASF SE, and Italian MIUR (funds ex 60%).

Supporting Information Available: Synthesis and characterization of compound **4**, MS and ^{1}H NMR spectra, optimized structure of **3**, crystal structures, temperature-dependent ^{1}H NMR spectra, selected bond lengths and POAV1 pyramidalization angles based on the optimized structures of **6** and **7**, a table with absolute energies, relative energies, MO energies, HOMO−LUMO gaps, and optical gaps of cis and trans conformations of **5**−**7**, comparison between computed frontier orbitals of **5**−**7**, complete ref 16, and the Cartesian coordinates of all the structures optimized. This material is available free of charge via the Internet at http://pubs.acs.org.